Optical Fiber Sensors from Laboratory to field trials : Application and trends at CEA LIST

Pierre Ferdinand, Sylvain Magne, Guillaume Laffont, Véronique Dewynter-Marty, Laurent Maurin, Cécile Prudhomme, Nicolas Roussel, Marie Giuseffi, Séverine Maguis

Fiber and Integrated Optics, 28:81–107, 2009

ISSN: 0146-8030 print/1096-4681 online
DOI: 10.1080/01468030802272559

Taylor & Francis
Taylor & Francis Group

Optical Fiber Sensors from Laboratory to Field Trials: Applications and Trends at CEA LIST

P. FERDINAND,[1] S. MAGNE,[1] G. LAFFONT,[1] V. DEWYNTER,[1] L. MAURIN,[1] C. PRUDHOMME,[1] N. ROUSSEL,[1] M. GIUSEFFI,[1] and S. MAGUIS[1]

[1]CEA, LIST, Laboratoire de Mesures Optiques, Gif sur Yvette, F-91191, France

Abstract *Fiber optic metrology developed at the CEA LIST laboratories involves fiber Bragg grating sensors, distributed Brillouin optical time domain reflectometry and optically stimulated luminescence dosimetry. Recent activities in optical fiber sensing are reviewed from laboratory experiments to field trials.*

Keywords BOTDR, DTS, FBG, OFS, Raman scattering, SHM

1. Introduction

From 1975, optical fibers developed for telecommunications have found parallel applications in the sensing area, taking advantages of their sensing properties. Striking examples at that time were the fiber optic gyroscope (FOG), the distributed temperature sensor (DTS), and the fiber optic hydrophone. All these developments aroused serious interests in optical fiber sensors (OFS) and many groups started works in the field early in the 1980s. The first international conference on OFS was held in London in April 1983.

OFS may make the engineer's job easier, as many usual transducers and sensors are sometimes bulky and do not lend themselves to multiplexing or remote measurements. For the most part, they cannot be used under harsh environments (high temperature, corrosive or chemically reactive atmospheres, explosion risk, shock or vibration, electromagnetic perturbation, or lightning).

The first optical sensors sold as products in the 1980s were temperature sensors (Luxtron, Accufiber, Vanzetti, York sensors, etc.). They involved various sensing mechanisms and were designed for several applications and ranges.

The driving force behind the development of any new sensor is the need for cheap, compact devices able to be used in industrial environments and with sufficient projected reliability to allow regular sensing or monitoring over a long period of time without intervention. This is exactly what happened 20 years ago for point temperature sensors [1] (e.g., fiber optic pyrometers). But, single-point transducers (i.e., the optical counterpart of

Received 18 March 2008; accepted 25 April 2008.
Address correspondence to Dr. Pierre Ferdinand, CEA, LIST, Boîte Courrier 94, Gif-sur-Yvette, F-91191, France. E-mail: pierre.ferdinand@cea.fr

a thermocouple or a platinum resistance thermometer) only seldom use the high intrinsic bandwidth of optical fibers. The need has therefore emerged to multiplex a number of sensing elements onto a single fiber and thus to create a distributed (or quasi-distributed) optical fiber sensor network (OFSN).

In 1989, a new spectral filter called fiber Bragg grating (FBG) has been presented [2], and shown to be simultaneously strain-, temperature-, and pressure-sensitive. This new device, obtained by photo-writing the core of an optical fiber using a UV laser light, led the way to many applications [3]. For instance, in the 1.55 μm window (C-band), spectral sensitivities of FBGs with respect to strain, temperature, and pressure are, respectively, $\sim$1.2 pm/(μm/m), $\sim$12 pm/K, and ~ -5 pm/MPa, slightly depending on fiber properties.

More recently, a distributed Brillouin sensing method based on optical time domain reflectometry (OTDR) reached the market after more than two decades of R&D. Recent progress in so-called B-OTDR (or B-OTDA) has been kicked off by the use of affordable fast modulators, powerful lasers and very high speed acquisition boards. B-OTDR instrumentations will probably be as common as DTS in a near future.

We attribute the growing use of OFS(N) to several intrinsic advantages that are put forward in a highly competitive market situation. Optical instrumentation advantages are partly due to intrinsic properties of optical fibers:

- electromagnetic interference (EMI) immunity,
- light weight,
- small size and flexibility,
- very low losses (long-span, some tens of kilometers),
- high temperature and radiation tolerance,
- stability and durability against harsh environments, and
- no local electrical power required at measurement points.

Other advantages are also due to the optoelectronic system:

- good metrological performances,
- multi parameter measurement and data fusion into a single parameter (wavelength),
- multiplexing capability (several sensors multiplexed on the same fiber),
- several fibers interrogated in real time,
- immunity to optical power light fluctuations,
- temperature-compensated measurement, and
- flexible sensing topology.

All these advantages are clearly of primary importance in distributed or quasi-distributed measurements. Today, OFS(N) are increasingly used anywhere where security or safety is concerned. To highlight the argument, let us list some examples: temperature and pressure sensors devoted to process control or safety are now advocated by the oil and gas industries; in electrical utilities optical fiber current sensors based on the Faraday effect are well known; in civil engineering as well as in composite material applications, the concept of structural health monitoring (SHM) based on FBG or B-OTDR becomes more and more a matter of concern for end users. Finally, DTS for fire detection are now deployed in many tunnels or critical infrastructures all around the world.

Concerning FBG-based sensors, one important way of innovation for end-users is linked to the possibility to design and photo-write FBGs of more complex patterns than those mostly used for telecommunications. Innovative FBG devices have been studied (blazed, Fabry-Perot, phase-shifted, etc.) with the aim of designing innovative filters for laser tuning, channel filtering, or improved detection (e.g., chemical or bio-medical).

Finally, FBGs are now evolving into the technology of photonic crystal fibers (PCF) where the grating structure is not only longitudinal but also transversal to create new guiding properties (dispersion, etc).

Activities of CEA LIST in fiber optic metrology were already described in previous articles [4–6]. This article reviews recent advances obtained at CEA LIST mainly with three dedicated techniques: FBG sensors, distributed B-OTDR, and OSL dosimetry. It focuses on specific applications dealing with several market sectors: structure monitoring in public works, railway industry, oil and gas, but also in (bio) medical sectors and will look at some recent developments and technologies, seeds of future innovations for sensing industry and of benefit for end-users.

2. OFS and SHM

Fiber sensing is increasingly used for structure monitoring (concrete, steel, composite) or composite material manufacturing. FBG-based quasi-distributed sensing seems relatively mature, as many structures worldwide have already been equipped with such sensors during the past ten years. Nevertheless, the market is not yet widely open for the optical fiber technology, in spite of few very big projects (e.g., bridge monitoring in China). On the other hand, B-OTDR- and DTS-based distributed sensors are attractive and complementary of former approach.

OFS for monitoring and safety may include an FBG-based local sensing when only discrete sensors are required, or Brillouin or Raman sensing (continuous measurements over multi kilometric range) when profiles are required.

2.1. FBG-Based Sensing

FBGs provide absolute measurement (wavelength-based encoding for both sensor identification and measurement). As the spectral signature renders the measurement free from intensity fluctuations, it guarantees reproducible measurements despite optical losses (bending, aging of connectors, etc.) or even under high radiation environments (silica darkening) [3]. It is linear in response, interrupt-immune and of very low insertion loss so that they can be multiplexed in series along a single mode fiber. Also, any specific network (star, series, and fish-bone) can be implemented and modified after set-up, thus increasing return-on-investment. Moreover, FBGs may be also embedded into materials (e.g., composite materials) to provide local damage detection as well as internal strain field mapping with high localization, resolution in strain and large measurement range. The FBG is therefore a major component for the development of smart structure technology. It offers the promise of undertaking 'real-time' structural measurements with built-in sensor systems expected to be cost-effective for a large number of multiplexed sensors.

2.2. OFSs Based on Reflectometry

Reflectometry is the optical equivalent of radar. A pulse of light is launched into the fiber that generates scattered light that is composed of Rayleigh as well as Raman and Brillouin spectral lines (Figure 1).

In usual OTDR technique, one looks at the Rayleigh backscattered signature (at the same wavelength of the laser). This signature gives information on losses, breaks, etc. along the fiber length. In that case, the fiber acts as both sensing element and transmission

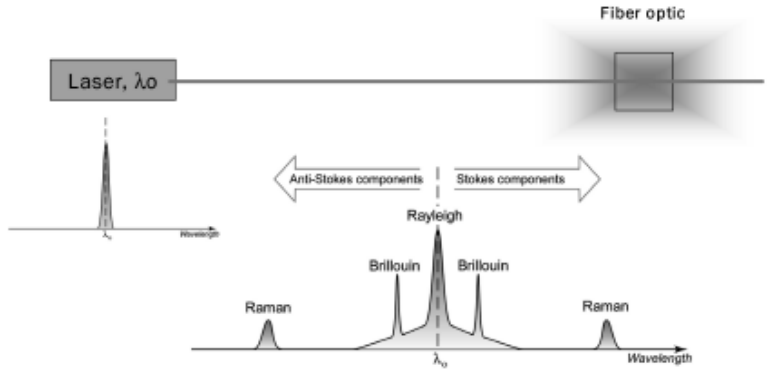

Figure 1. Scattering phenomena in optical fibers. (Courtesy of OMNISENS.)

medium. The range of telecom-type OTDRs is kilometric and the spatial resolution is typically 1 m (corresponding to 10 ns pulses and 100 MHz electronic bandpass). OTDRs based on photon counting (100 ps pulses) exhibit a centimetric resolution but a more limited range (some 100 m).

2.2.1. Brillouin-Based Sensing. Brillouin scattering results from the Bragg diffraction of light by acoustic waves. Any acoustic wave induces a periodic modification of the refractive index, which develops a diffraction grating. Due to Doppler effect, a frequency shift $\Delta\nu_B$ (proportional to the acoustic speed in the medium) is induced by the grating. At any location along the fiber, $\Delta\nu_B$ is proportional to temperature and strain variations. Figure 2 shows the Brillouin gain spectrum for each frequency shift vs. distance. When the optical fiber experiences traction (resp., compression), $\Delta\nu_B$ shifts to higher (resp., lower) frequency.

The performance of spontaneous Brillouin-OTDR is low since only a ppm fraction of light power is backscattered; hence, this technique requires averaging over a long period of time.

Stimulated Brillouin back scattering has been studied with the aim to improve both signal-to-noise ratio and response time. In this case (called Brillouin-OTDA), two contrapropagative optical signals are launched into the optical fiber (through both ends). One continuous wave (CW) signal (pump) is kept fixed in frequency, while the second one (probe) is pulsed and frequency-tuned over a range depending on the user's specifications. When the frequency difference between pump and probe equals $\Delta\nu_B$, the probe signal gets amplified.

Once the B-OTDA system is calibrated, both temperature and strain profiles may be monitored along a single optical fiber. A common reference is an acrylate-coated fiber in a stable environment for which strain and thermal sensitivities are 50.5 kHz/(μm/m) and 1 MHz/K. B-OTDA performances are listed in Table 1.

2.2.2. Raman-Based Sensing. Raman scattering results from the interaction between an incident light and vibrations of the molecules present in the propagation medium. As for Brillouin signal, a Raman signal comprises a Stokes spectral line (the molecule absorbs a part of photon energy) and an anti-Stokes line (the molecule transfers a part

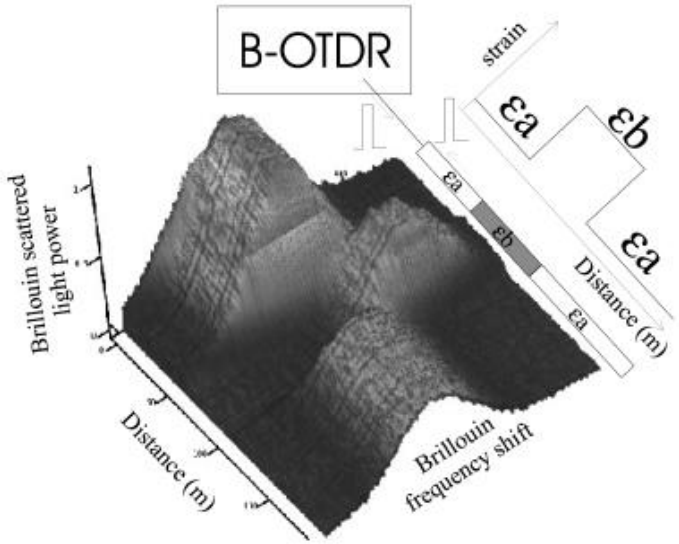

Figure 2. Brillouin gain and frequency shift vs. distance of a partially strained optical fiber.

of its energy to the scattered photon), both shifted in wavelength from the Rayleigh one. Differently to the Brillouin effect, the frequency of the backscattered light is not affected by environmental conditions and only spectral intensities are taken into account. The intensity of the anti-Stokes spectral line depends on temperature while the intensity of the Stokes line does not. A temperature profile is then obtained by normalizing the anti-Stokes OTDR profile by the Stokes OTDR profile. The DTS is thus immune to any change in light transmission (losses, laser power fluctuations, etc.) or electronic gain instability. A location along the fiber of the temperature reading is determined by measuring the time-of-flight of the signal, similar to a radar echo. State-of-the-art DTS systems present a spatial resolution of roughly 1 m and a temperature resolution of about 0.1°C.

Table 1
Performances of the B-OTDR device

Parameter	Value
Strain accuracy (temperature)	10 μm/m (1°C)
Strain repeatability (temperature)	±5 μm/m (±0.5°C)
Spatial resolution	>0.1 m
Measurement time	Typ. 1 min
Distance range	Some tens of km
Strain and temperature ranges	±1.25% (±600°C)
Dynamic range	>20 dB

Courtesy of Omnisens.

3. Some SHM Applications

SHM is now an important application field for optical sensors. The SHM community shows a growing interest to FBG sensors and systems, with almost one-third of scientific publications ranging from naval to railway and aerospace applications [7]. FBG sensors have been commercially available for years thanks to the telecommunication market needs, and several companies are now selling monitoring systems dedicated to FBG sensors metrology, making this technology accessible for routine strain and temperature measurements.

3.1. *SHM for Trains*

3.1.1. Fatigue Tests Monitoring of a Composite Blade for Train Bogies. Some applications may require specific developments from the sensor point of view since the FBG wavelength depends on several factors. It is therefore necessary to separate several contributions, and usually, strain measurements require two closely located FBGs whereas temperature measurements may require only one grating. These requirements are often very stringent for the sensors design. Restricting factors are micro-bending attenuation losses or mechanically-induced weaknesses due to fiber embedment, especially in composite materials.

For example, spring blades made of organic composite material are likely to be used in future train bogies as a replacement of conventional steel-based bogies. In collaboration with Alstom (French high speed train 'TGV' manufacturer), the CEA LIST has equipped a composite spring blade with FBG sensors (Figure 3) and performed standard fatigue qualification tests (7 Hz force cycling and temperature cycling during three weeks). The optical fiber was embedded into the composite blade during the manufacturing process between two fiber-reinforced layers. The FBG-based temperature sensor required to compensate for the temperature sensitivity of FBG strain sensors has not been embedded inside the blade under test to prevent delamination, but into a dummy part of the same material submitted to the same temperature cycling. FBG strain measurements have demonstrated in these conditions their reliability during more than 10^7 cycles, surpassing the traditional electrical strain gages, which failed at 4.10^6 cycles [8].

3.1.2. Smart Trains and Infrastructures. Today, Europe is facing the challenge of shaping an improved railway system for the 21st century in order to address the future increased needs and demands for European citizens' mobility. As both passenger and freight traffics will strongly increase in a near future, the European Commission is launching research initiatives in order to achieve a better interoperability between the rolling and standing stock companies in a deregulated market, hence confirming its essential role in a sustainable European-scaled transport system.

In this frame, today's developments on monitoring systems and sensors at CEA LIST can be illustrated by two EU-funded projects: 'Smart Monitoring In Train Systems' (FP5-SMITS) and 'CATenary InterfacE MONitoring' (FP6-CATIEMON), dedicated to the high-speed monitoring of the interface between a pantograph's train and its overhead contact line (OCL) in terms of impacts, vertical contact force, and OCL position onto the pantograph.

The very stringent specifications both in terms of frequency (1 kHz), precision, resolution (~1 pm in wavelength), and number of sensors, have led our laboratory to develop a new monitoring system generation based on a high speed spectrally tunable source [9] and an internal wavelength reference for absolute wavelength measurements.

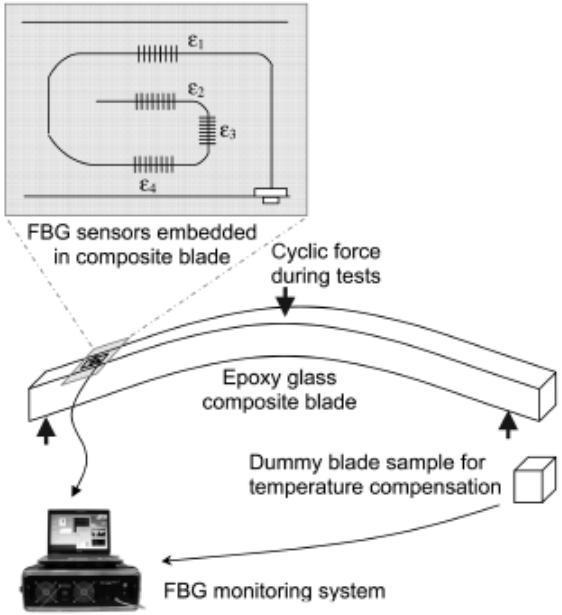

Figure 3. Fatigue testing of a composite bogie. Climatic chamber conditions: temperature cycling, sinusoidal force applied at 7 Hz, 16.10^6 cycles.

On the other hand, a 'smart' pantograph with embedded FBG sensors has been developed within the SMITS consortium (Siemens, Morganite, SNCF, IPHT, CEA LIST, BLS).

This monitoring system has been integrated into an existing measurement loop with standard electrical sensors into a very high speed TGV train, delivering vertical forces, temperature, and OCL position measurements data in real time during more than 6,000 km at 300 km/h between Paris and Vendôme (France). This field test demonstrated the ability of FBG sensors for accurate monitoring measurements in a high voltage environment (Figure 4) [10].

Within the same framework, the CEA LIST also took part in the CATIEMON project. This second project aimed at improving the reliability, availability, and interoperability of cross boundaries and independent infrastructure networks. Innovative sensors and monitoring tools are required in order for both rolling stocks operators and infrastructure managers to optimize maintenance costs. To achieve this, the interaction between pantographs and catenaries (or contact wires) must be monitored both for train operators and network managers in order to avoid excessive wear of their equipments. While the previous SMITS project was dedicated to the monitoring of the interaction between the pantograph and the OCL, the CATIEMON project aimed at developing an inspection gate integrating several kinds of sensors in order to monitor several useful parameters such as the uplift of the wire (in three dimensions) and the local strain along the catenary. In the context of high speed passenger and freight trains, FBG-based displacement, strain and hit detection sensors are particularly well-suited due to their intrinsic electro-magnetic

(a)

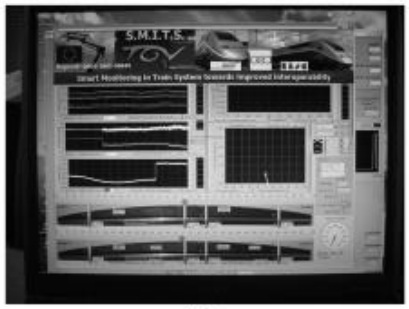

(b)

(c)

Figure 4. (a) TGV Pantograph model (Faiveley CX25) in contact with the OCL when running. (b) SHM remote supervision screen during TGV field trial. (c) Detail of the FBG-based leading fiber on pantograph head.

(EM) immunity and their low intrusivity. These sensors have been installed at the closest location to the pantograph-catenary interaction (i.e., very close to the contact wire). Moreover, FBG have been bonded at several locations along the OCL using a single fiber (simplified network topology).

Interrogation units dedicated to FBG monitoring have been specifically developed for this project in order to fulfil the end-users needs for high speed (from 1 kHz up to 1 MHz) and multichannel wavelength-referenced monitoring tools. They have been used to perform remote detection of the FBG sensors thanks to the low attenuation properties of the fiber used (standard telecom fibers). All these sensors and systems have been successfully installed and tested during several field tests. The measurements are currently being processed and analyzed.

3.2. Oil and Gas Applications

3.2.1. FBG and DTS Raman in Oil and Gas. Fiber optic sensors are used in the oil and gas industry because of their robustness in harsh environment and their small dimensions (non intrusive and flexible). Furthermore, the optical sensors are passive (no power electronics) and fibers may be deployed on very long spans (some tens of kilometers). A great number of sensors and parameters may be monitored simultaneously (strain, pressure, temperature, etc.) with a single instrumentation. In case of offshore monitoring (Figure 5), the measurement system is located on a platform (e.g., floating production storage and offloading [FPSO]).

Today, major oil companies are in demand of real-time and permanent monitoring of various parameters, especially in offshore where the environmental conditions are harsh and where the maintenance is difficult and very expensive. The objective is to optimize oil production under safe and environmentally protective conditions. DTS Raman is a measurement technique widely used by companies such as Weatherford or Sensa.

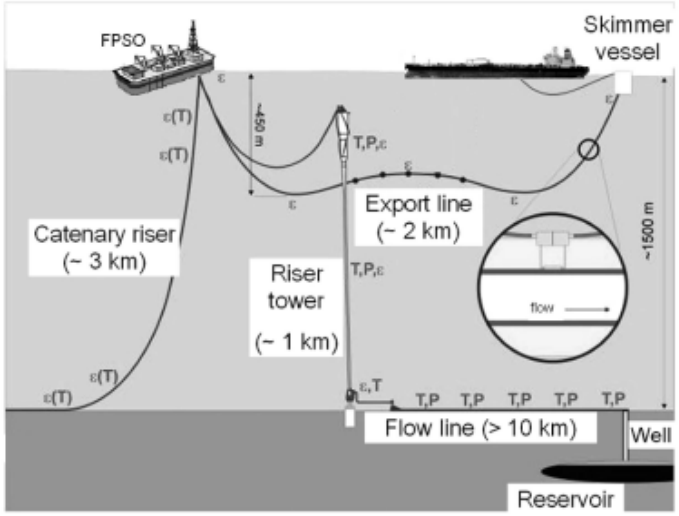

Figure 5. Standard offshore installations for oil production.

Let us mention a few applications and how FBG-based sensors, and DTS are used.

Health monitoring of the pipeline structure: The objective is to monitor strain and pressure supported by the pipelines, and to assess axial stress and bending. This allows fatigue damage to be estimated. This fatigue monitoring prevents unnecessary pipeline intrusions or expensive shut down operations by regularly checking the health of the whole structure. This kind of measurement also enables the operator to identify various potential threats to the health of the pipeline and detect changing conditions caused by earthquakes, above ground vehicles, and other events that may result in pipeline failure. Failure locations can be identified very easily and so the expense of on-going maintenance is reduced.

Flow-control (slug detection): Real time pressure and temperature measurements provide indications on the fluid flow inside the pipeline. Slug detection is an important challenge for oil companies as it is a growing problem (delays in production time and volume). Operators can exploit the full capacity of the plant when the flow is stable. Therefore, early warnings about slugs would enable the operator to adjust the flow when they occur.

Prevent gas hydrate formation: In some thermodynamic conditions, gas hydrates may form and block the pipeline. By monitoring pressure and temperature in real time, the operator would be able to prevent from hydrate formation and thus avoid unnecessary shut down.

As explained above, real-time monitoring of structures is a new and specific need. Conventional sensors are still used but their lifetimes are short and their reliability is not satisfactory in harsh conditions (especially in deep offshore fields). OFS, and in particular, FBG sensors, are used increasingly by oil companies.

3.2.2. FBG Applied to Riser Monitoring. A French project involving the CEA LIST, the IFREMER, TOTAL, ACERGY Group, and CYBERNETIX, consisted of developing FBG sensors and the associated measurement system, for the simultaneous determination of the temperature, strain, and pressure at different locations around the surface of a pipeline. The objective is to control the fluid flow (flow rate, slug detection) and to monitor pipeline fatigue.

FBG can be arranged in a specific way to form a "rosette," developed and patented by the CEA LIST. In our application, it is composed of three FBGs. A first one, located along the principal axis of the pipeline, is sensitive to the axial strain of the structure, and therefore to flexion or traction efforts.

The second one, positioned along the transverse axis of the pipeline, is used to determine essentially efforts induced by internal pressure variations of the pipeline. The last one, isolated from strain, is dedicated to temperature measurement; it is used to directly monitor the oil production but also to compensate for the temperature effect on the two other gratings. In practice, a matrix calculation is necessary to get the two strain parameters (axial strain and bending-induced strain). Furthermore, by arranging three rosettes placed at 120°, one from each other along the circumference of the pipeline, we also get the magnitude of the bending and its orientation with respect to the pipeline. For an easier positioning of the rosettes on the pipeline, the sensing fiber (with the Bragg gratings) is deployed on a Kapton® sheet (Figure 6).

The project allowed us to validate some critical aspects, due to harsh environmental conditions:

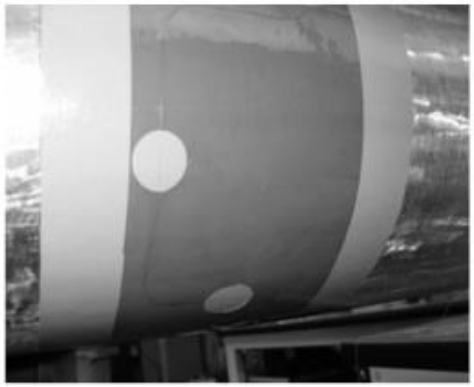

(a)

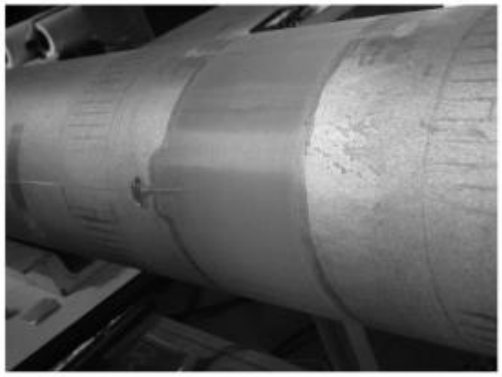

(b)

Figure 6. Rosette patch used for strain measurement on (a) pipeline and (b) packaging.

Design and realization of the patch "rosette": Great care must be taken to choose the different components, the optical fiber and Bragg grating (recoating, Kapton® type). A dedicated design and fabrication procedure have been developed that take into account FBG alignment, patch/structure interface, specific fiber output of the patch (water-tightness), and Bragg grating packaging used for the temperature measurement.

Coupling the patch "rosette" on the structure: A bonding procedure has been tested (polymerization and heating onto the pipeline) and the performance of the bonding joint has been tested in a climatic chamber in a high temperature environment.

Tests in hyperbar conditions: The instrumented pipeline has then been tested in a hyperbaric chamber (up to 300 bar). The FBG sensors performed well under high pressure (equivalent to 3,000 m in depth).

This rosette patch will be validated in representative conditions (submarine environment, high temperature and pressure) before being used on field production.

3.3. *Smart Civil Engineering and Public Works*

The construction and maintenance costs of civil structures and infrastructures represent at least 10% of the public investment in most western countries. Many tunnels and bridges built some decades ago need maintenance and, in many cases, an extension of their capacity and life-time. Today, managers of civil infrastructures are facing the challenge of maintaining infrastructures in good 'health' with minimum perturbations during normal use, spending a limited budget. Such an option is less expensive than building new structures but it is more complicated since it requires new management instruments.

SHM based on sensor networks that monitor the relevant mechanical parameters of a structure behavior is certainly one of these new instruments that are gaining importance in the civil engineering domain. Traditional sensing technology based on electrical transducers (vibrating wires, inductive displacement sensors, etc.), is able to measure the most needed parameters. Nevertheless, OFSs have recently done significant entrance in this sector, due to attractive advantages.

3.3.1. Civil Engineering. Many civil structures, such as bridges, have been built in the middle of the last century and reach a similar level of degradation accelerated by loading conditions and corrosion. In Europe, both National Authorities and the European Commission promote Health Monitoring concepts, instrumentation of existing structures, and help in the design of new durable structures of higher performance. Many projects dealing with bridge monitoring have been lead during the last decade in Europe, North America, and now in China.

Many civil structures are likely to be instrumented with OFS and FBGs (historical monuments, box-girder bridges, cable-stayed bridges, dams, large buildings, tunnels, etc.). Applications include in-situ concrete curing process monitoring and pre-stress determination, repair using epoxy-bonded carbon fiber reinforced panels (CFRP), health monitoring (micro-cracking, impact detection, post-seismic damage evaluation), steel corrosion detection, load rating, weight-in-motion (WIM), and vehicle counting/ identification (VC/Id). These applications have been described in previous reviews, and many civil engineering structures have already been equipped by OFS, mainly FBGs and white light interferometers, for instance.

In this context, the CEA LIST equipped in 2001 the Saint-Jean Bridge in Bordeaux, France with 11 spectrally multiplexed FBG-based extensometers, several FBG temperature sensors, and an acquisition unit. The purpose was to check the reliability and user-friendliness of its instrumentation with the help of the French LCPC (in charge of civil engineering surveillance in France) that provided usual electrical strain gauges for comparison.

A standardized loading of the bridge has been performed, with the purpose of correlating its mechanical reaction to loading conditions. Moreover, the equipment has been operating for one year to take into account the winter-summer cycle [11].

3.3.2. Underground Monitoring. In the context of the European FP6-TUNCONSTRUCT project, the CEA LIST is proposing an innovative method combining Brillouin-OTDA and a special cable design to monitor settlements during tunnelling works in urban environments, especially with tunnelling boring machine (TBM). The challenge is to avoid confinement losses, which remain an important risk for public works, leading to additional delays and costs and to higher insurance costs. In this particular application,

usual surface instrumentations cannot be set up because of high building density in many overcrowded cities. In such areas, the tunnelling boring machine has to deal with the challenge of keeping the surface undisturbed.

The original approach consists of an early detection of the settlement occurring close to the tunnel vault, before it propagates up to the surface. It requires a directional drilling (HDD) along a chosen axis (Figure 7), the borehole trajectory being parallel and above the future tunnel axis.

The sensing cable will be deployed inside the borehole between the upper part of the tunnel (typically 2 m above the vault) and the surface (Figure 7). The sensing cable is able to monitor axial strain and bending-induced strains. The profile of bending radius and orientation with respect to a ground reference are obtained from bending-induced strain profiles obtained from B-OTDA measurements.

When the cable is bent, the upper fibers are compressed while the lower fibers are submitted to traction. In this underground application where the fiber positioning is unknown, the cable is composed of 3 parallel optical fibers placed at several orientations along the cable cross-section (Figure 8). For the sake of simplicity, an angle of $2.\pi/3$ is chosen but other arrangements are possible.

Let us consider a cable of diameter ϕ submitted to a curvature radius R. The bending-induced strain is then: $\varepsilon_{c\max} = \frac{\phi}{2R}$. Let ε_{fa}, ε_{fb}, and ε_{fc} be the bending-induced strains experienced by fiber a, b, and c, respectively. The strain applied to each fiber (a, b, c) depends on the curvature radius R, the bending orientation ψ, and axial strain ε_a as follows:

$$\varepsilon_{fa} = \varepsilon_a + \frac{\phi}{2R}\cos(\psi) + Temp$$

$$\varepsilon_{fc} = \varepsilon_a + \frac{\phi}{2R}\cos\left(\psi - \frac{2\pi}{3}\right) + Temp$$

$$\varepsilon_{fb} = \varepsilon_a + \frac{\phi}{2R}\cos\left(\psi + \frac{2\pi}{3}\right) + Temp.$$

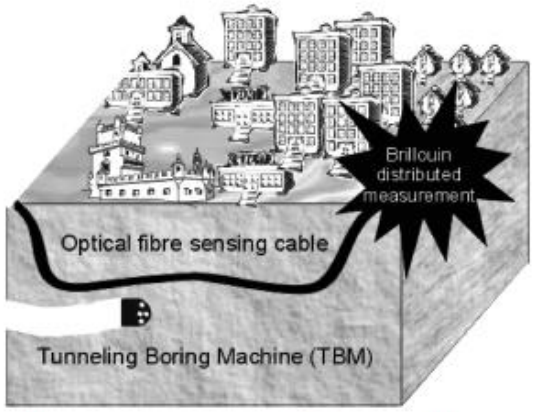

Figure 7. 3D artist view of underground Brillouin-based SHM while tunnelling.

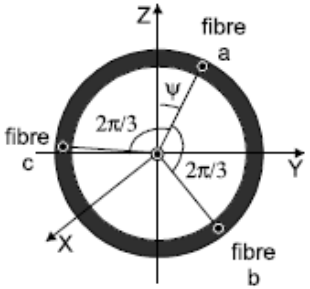

Figure 8. Section of '3D' Brillouin sensing cable (CEA LIST patent).

The temperature and axial strain are similar for every fiber. Only the bending-induced strains are fiber-dependent. Therefore, a simple trigonometric calculation leads to the value of the bending-induced strain:

$$\varepsilon_{c\max}(x) = \sqrt{\frac{1}{3}(\varepsilon_{fb}(x) - \varepsilon_{fc}(x))^2 + (\varepsilon_{fa}(x) - \varepsilon_a(x))^2} \quad \text{with} \quad \varepsilon_a = \frac{\varepsilon_{fa} + \varepsilon_{fb} + \varepsilon_{fc}}{3}.$$

Then, it is possible to retrieve the curvature profile from the strain profile using the following equation:

$$\frac{1}{\rho(x)} = \frac{2\varepsilon_{c\max}(x)}{\phi}$$

The settlement profile $z(x)$ may be estimated by integrating twice the strain profile (i.e., the inverse of the curvature profile $\rho(x)$. A dedicated algorithm has been perfected by the CEA LIST to optimize the integration.

A first prototype of industrial cable has been manufactured and qualified. In the following example the cable is submitted to an "S" curve (Figure 9).

The result of the integration is then compared to the experimental settlement arbitrarily set onto the cable and the adjustment proves satisfactory (Figure 10).

4. Medical and Biomedical Applications

4.1. Multichannel Fiber Optic OSL Dosimeter

Optically stimulated luminescence dosimetry (OSLD) is investigated at CEA LIST since 1995 for radiation protection (RP) of workers and dismantling of nuclear installations [12, 13], benefiting from flexibility and remote operation provided by optical fibers. Since 2004, the CEA LIST is involved in the European FP6-MAESTRO Project and collaborates with the Institut Gustave Roussy (IGR), one of the biggest cancer treatment centers in Europe [14]. The aim is to design and test an optical fiber dosimeter for the on-line in-vivo quality control of the dose in radiotherapy (RT), likely to be a legal requirement in a near future. Complex RT techniques (such as intensity-modulated RT [IMRT]) involve high-dose gradients and several beam orientations from the accelerator. The conformity of the dose distribution to the tumor is greatly improved and leads to a reduced dose to surrounding healthy tissues and critical organs, but in return requires an accurate

Figure 9. Experimental set-up for '3D' cable bending calibration.

dosimetry and a large number of sensors. Most RT treatments involve several dose fractions of typically 2 Gy and absorbed doses are measured after treatment (i.e., after irradiation) during inter-patient time. Finally, some patients may also receive radiation of their entire body, also called total body irradiation (TBI) in preparation for a spinal cord cell transplant. TBI treatments require a real-time estimation of the cumulated dose (to provide feedback to the physician during treatment).

Principle of OSL. OSLD is similar to the well-known thermoluminescence dosimetry (TLD) except that the luminescence is stimulated by light instead of heat, opening the way to a remote and operational fiber optic (FO) interrogation. During irradiation, a fraction of the electrons are promptly recombined and generate RL (radioluminescence). Others are trapped at defect sites in the crystal lattice and remain stored for undetermined periods of time. Electrons are released on request by a laser light and produce an OSL that decays as the trap levels are emptied. The stimulation spectrum is related to trap centers and the OSL spectrum is related to recombination centers. Since the stimulating wavelength is longer than the OSL wavelength, the OSL does not overlap with usual Stokes fluorescence. The integration of the OSL signal is proportional to the dose absorbed by the OSL material between two successive stimulations. The time decay of the OSL is inversely proportional to light intensity ($W.m^{-2}$) and also depends on laser wavelength with respect to the stimulation spectrum.

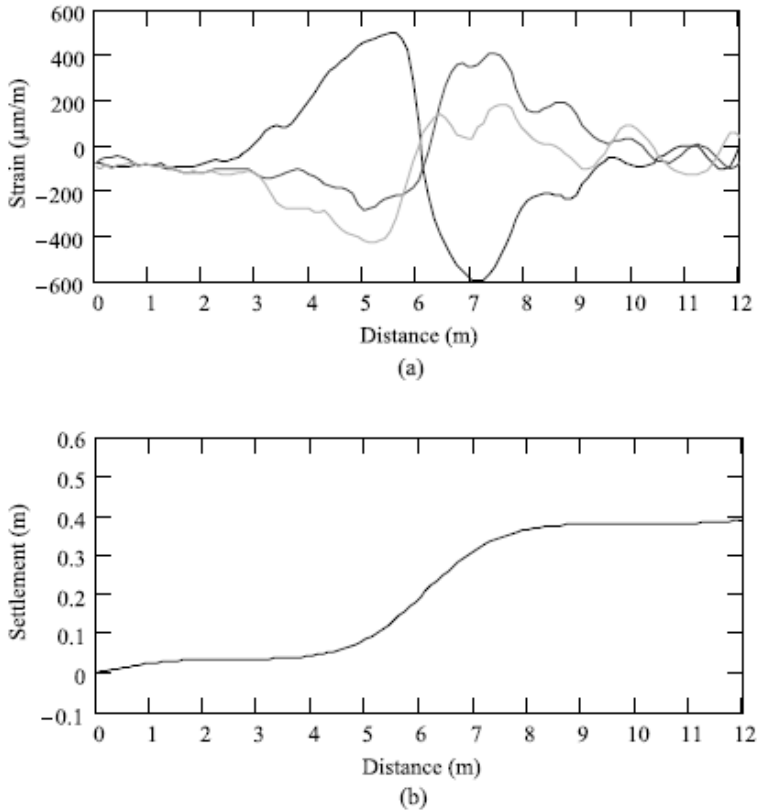

Figure 10. (a) Three-fiber Brillouin strain profiles ε_{fa}, ε_{fb}, and ε_{fc}. (b) Settlement profile calculated by double integration of ε_{fa}, ε_{fb}, and ε_{fc}.

Advantages of a FO OSL/RL dosimetry. FO OSL dosimetry conveys a lot of advantages with respect to usual techniques (diodes, MOSFETS, TLD). It provides a remote point monitoring of both dose and dose rate (or cumulated dose) under operation (i.e., no sensor collection is needed as for TL). Alumina crystal fibers were chosen as detectors because they show insignificant fading at room temperature and can be used both as integrators (OSL) or scintillators (RL). They are cheap, small (mm^3), optically transparent, and not hygroscopic. The fiber sensors exhibit low temperature, angular, and energy dependencies. Furthermore, they are nearly radiation transparent since the Z of alumina is low (10), they are made of polymer materials and do not incorporate any metallic part (no electric wire). Finally, they are immune to electromagnetic perturbations (fiber optic technology) and are compatible with medical applications (sterilizable).

FO-OSL/RL dosimetry is expected to provide both simplification in the treatment procedures and significant cost reduction associated to calibration and sensor replacement (actually performed by high-skill personnel). In the perspective of an on-line in-vivo

dosimetry, it is of prime importance to reduce the cost associated to these time-consuming tasks. OSL dosimetry may be a valuable solution because: (i) the sensor lifetime is potentially very important (several years, i.e., much longer than MOSFETs); (ii) few correction factors should be dealt with (by comparison to diodes); and finally, (iii) the whole medical data associated to a great number of sensors and patients should be stored and analyzed in a single system (user-friendly man-machine interface). The OSL system should provide gains in maintenance cost and simplification in data handling which render it attractive on long-term on the basis of a return-on-investment (ROI) taking into account both purchase and maintenance costs.

Optically stimulated luminescence (OSL) dosimetry system. A multichannel OSL fiber optic dosimeter based on alumina crystals as detectors has been developed for the first time by the CEA LIST. The OSL dosimeter system of the CEA LIST (Figure 11) works in continuous-wave (CW-OSL). This operating mode is simple and convenient for achieving delayed OSL measurements after RT, IMRT, or TBI treatments. Moreover, the system incorporates a 16-channel optical fiber switch that provides a cost-effective sensor interrogation. This instrumentation will be located in a control room (next to the irradiation room), handled by a laptop through dedicated software written in LabVIEW®. Each OSL fiber sensor consists of an optical cable with a SMA connector at one end and a molded cylindrical head at the other. The radiation-transparent head protects the α-Al_2O_3 crystal ($\varnothing = 1$ mm, 1 mm long) affixed near the end of a silica fiber.

Every OSL sensor is remotely stimulated via an optical fiber ($\varnothing = 600$ μm, $NA = 0.37$) using a diode-pumped solid-state (DPSS) laser (@ 532 nm, 200 mW) and bleached for a next usage. The OSL is collected and guided back along the same fiber to a photomultiplier tube through adequate optical filters. OSL signals are read sequentially after treatment (during inter-patient time), corrected for background noise, and integrated to provide the absorbed doses delivered during the treatment. The dose resolution of our system is ~1 mGy and the response time is less than 20 seconds (25 mW laser power). The calibration curve shows a sub-linearity behavior that is accurately fitted with a quadratic equation.

Figure 11. OSL/RL dosimeter developed by the CEA LIST.

During TBI treatments, the RL signals emitted by the sensors would be time-sampled by the optical switch and a routine calculates the dose rate for each sensor. The part of Cerenkov light from the fiber ("Stem effect") has been found to be second-order in the RL signal with respect to the scintillation part localized in the alumina crystal, and thus, can be compensated for by a reference fiber.

Tests in pre-clinical conditions on body simulators (phantoms) have shown satisfactory behavior in dose repeatability and reproducibility. These tests are still going on until 2009 and will also check the compliance of the OSL system with the medical specifications.

Besides RP, RT, and dismantling of nuclear installations, other applications are concerned with this innovative technique. FO OSL/RL dosimetry may be used in radiology, in reactor monitoring and safety (for power plants or submarines), in nuclear storage sites, and in process control (food irradiation, composite polymerisation).

4.2. *Innovative Technologies for Sensing: Slanted FBG and FCP*

Slanted or tilted FBGs consist of a periodic modulation of the fiber core's refractive index but this modulation is tilted with respect to the fiber propagation axis. This is easily achieved with conventional photo-writing set-ups such as those involving phase masks or Lloyd mirror interferometers by introducing an angle between the fiber and the UV-light fringe pattern. Even small angles drastically change the spectral response of the grating and also, as described hereunder, the sensing properties.

Figure 12a presents transmission spectra of Tilted Fiber Bragg Gratings (TFBGs) photo written in standard single-mode fiber. Figures 12b and 12c show the change in TFBGs spectral response when the tilt angle θ increases. For $\theta = 0°$, the dominant coupling occurs between the forward-propagating and backward-propagating guided modes (i.e., so-called Bragg resonance). Resonances below 1538 nm correspond to the coupling between the fundamental mode (forward-propagating guided mode) and backward-propagating cladding modes (Figure 13). The coupling coefficient between the fundamental and backward cladding modes is not null because the grating is spatially localized in the core. As the tilt angle increases, the coupling coefficient between forward-propagating and backward-propagating guided modes decreases. As a consequence, the Bragg reflectivity decreases as well. The greater the tilt angle θ, the greater the coupling to cladding modes. The optimum coupling is obtained for higher-order modes. On transmission spectra, one may notice that one resonance out of two exhibits slightly lower amplitude. These resonances with lower amplitude result from coupling between the fundamental guided mode and LP1n cladding modes, the other resonances (with higher amplitude) are due to coupling between the fundamental guided mode and LP0n cladding modes.

In the case of Figure 12, external medium is air ($n = 1$). Now, let us consider the 16°-tilted TFBG, surrounded by an external medium of refractive index n_{ext}. For n_{ext} between [1, 1.296], the spectrum shape is almost the same than for the 16°-tilted TFBG, only a small red shift of the resonances can be observed. For $n_{clad} > n_{ext} > 1.296$, we notice a gradual disappearance of the resonances composing the spectral response in transmission (Figure 14), from low wavelength resonances to high wavelength resonances. The forward-guided mode is then not only coupled to the backward cladding modes but also to the continuum of radiation modes. When n_{ext} reaches the cladding refractive index value (n_{clad}), cladding modes are not guided anymore, as the interface between the cladding and the external medium disappears. Only the coupling between the forward-

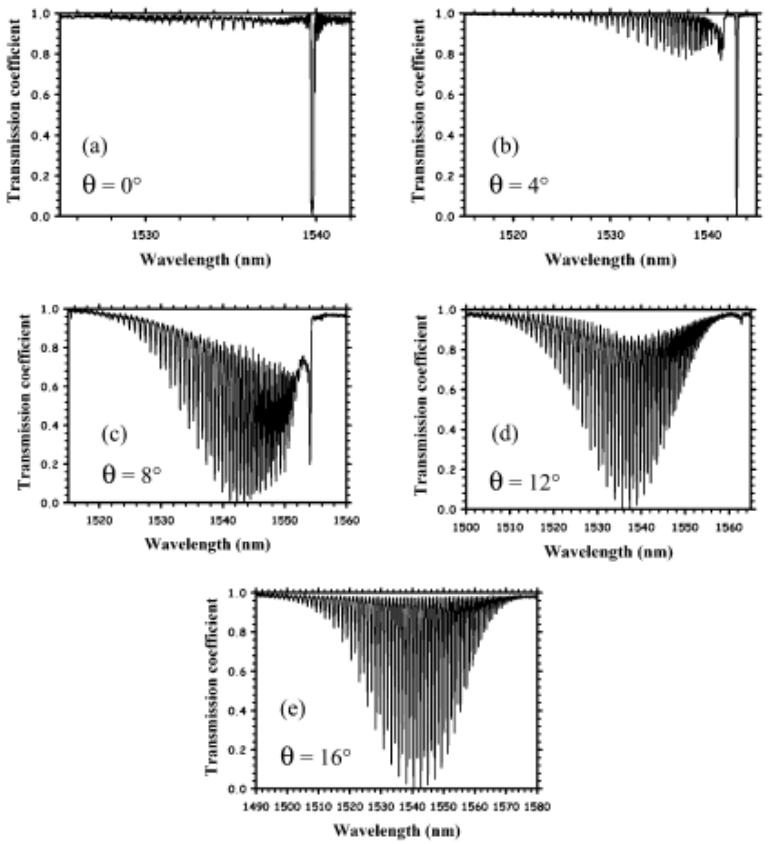

Figure 12. Transmission spectra of (a) non-tilted, (b) 4°-tilted, (c) 8°-tilted, (d) 12°-tilted, and (e) 16°-tilted FBGs photo-written in telecom single-mode fiber with a Lloyd interferometer set-up.

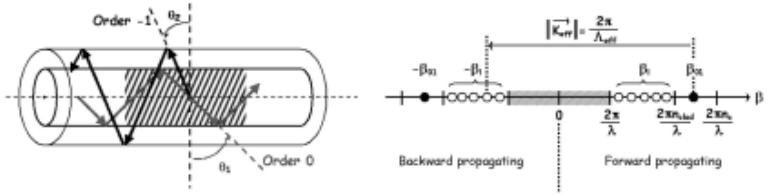

Figure 13. Left: Coupling between the fundamental mode (forward propagating guided mode) and backward cladding modes induced by TFBG. Right: Fundamental forward-propagating mode coupling to a backward-propagating cladding one ($\Lambda_{eff} = \Lambda \cos\theta$ is the effective grating period).

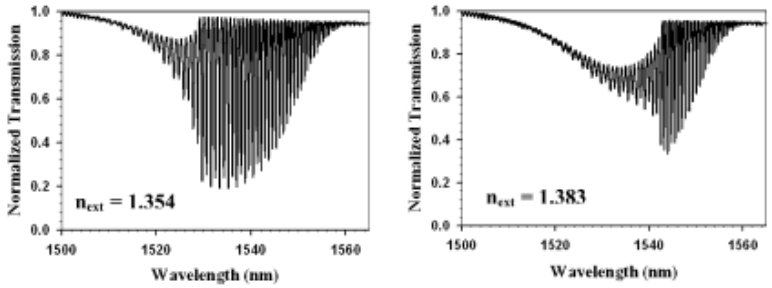

Figure 14. Transmission spectrum of a 16°-tilted FBG photo written in a standard single-mode fiber and for two distinct values of the surrounding refractive index.

guided mode and the continuum of radiation modes occurs. The TFBG spectral response in transmission is then a smooth envelope profile.

Based on this analysis, when n_{ext} varies, it is the global shape of the TFBG spectral response that is considered for sensing applications rather than the wavelength shift of a given spectral resonance [15, 16]. When next increases, with $1.3 < n_{ext} < n_{clad}$, the area delimited by the upper and lower envelope curves decreases. So, once area variations are calibrated with respect to refractive index values, such a grating can be used for sensing purposes. Moreover, since the Bragg spectrum shape is weakly affected by temperature, the temperature-sensitivity of the FBG-refractometer is very low ($<2.10^{-5}$ r.i.u./°C) and easily compensated.

Refractometers based on this principle are achieving resolution of 10^{-5} for refractive index values in the range [1.3, 1.45]. They have been used in cure monitoring of resins for composite manufacturing applications for instance. Such components may also find applications in biophotonics. Detection of target molecules such as proteins first need the additional development of specific fiber coating. Such transverse developments require skills not only in metrology and guided optic but also in research fields such as surface bio-functionalization and characterization.

The bio-functionalization consists of depositing a sensitive bio-film. It is the main issue in order to develop various kinds of optical biosensors. A tilted FBG is appropriate to measure any change in the refractive index of the external medium surrounding a traditional single-mode optical fiber. If a bio-film incorporating a selective probe molecule (e.g., a protein) coats on the external surface of a TFBG, the optical properties of the coating are modified by the capture of the target molecule (e.g., an antibody). The optical transduction is performed through refractive index measurement characterizing the interaction of the target molecule with the bio-film. The bio-functionalization, i.e., the formation of the bio-macromolecular film onto an optical fiber involves two steps. An intermediate polymeric layer or multilayer is formed on the silica wall before the immobilization step of the probe bio-molecule to avoid non-specific interactions between the probe, the target bio-molecules and the surface.

A strategy consists of the production of self-assembled polyelectrolyte layers assembled via electrostatic interactions. The electrostatic self-assembled film deposition method is based on the electrostatic attraction between oppositely charged molecules in each monolayer deposited, and involves several steps. First, the optical fiber is treated in a 1 M NaOH solution for 30 minutes to create a negatively charged surface. Then, the substrate is dipped alternatively into cationic polymer (polycation) and anionic polymer

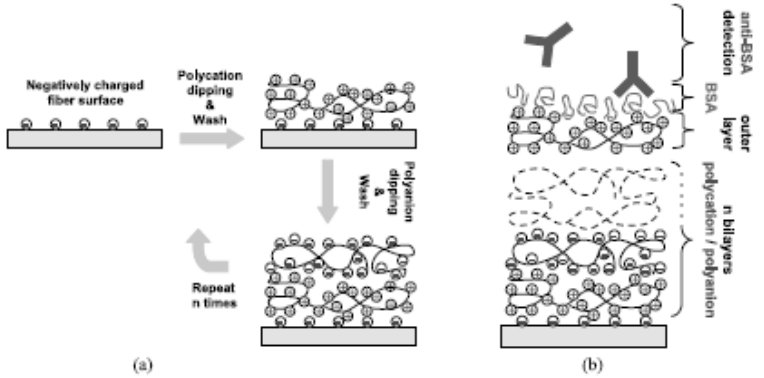

Figure 15. Schemes of (a) self-assembly process and (b) BSA antibodies binding to the immobilized BSA.

(polyanion) solutions in order to create polyelectrolyte multilayers (Figure 15a). Then, a charged protein (e.g., the bovine serum albumin [BSA]) can be adsorbed by electrostatic interactions to the oppositely charged fiber surface (Figure 15b).

The process of bio-functionalization resulted in variations in the refractive index in the vicinity of the fiber surface, which were monitored with the TFBG-based sensor. To control the surface coverage of the BSA, the surface morphology of the deposited film is monitored with atomic force microscopy (AFM). These measurements allow the reconstruction of three-dimensional images of the topography of the scanned surface. In the resulting images of the functionalized surface, we observe aggregation patterns characteristic of proteins, which demonstrates that the BSA protein is effectively attached to the surface.

The binding of target molecules (see Figure 15b), i.e., BSA antibodies, to the immobilized BSA was observed in real time for several antibody concentrations; the higher the antibody concentration, the greater the biosensor response in terms of refractive index variations. For these reasons, the TFBG-based biosensor seems to offer a new means of directly measuring antibody levels.

This technique, though still in its early stages of development, seems promising as it makes it possible to consider the realization of a new kind of biosensors and is relatively simple to implement. Nevertheless, long-term stability of coatings at high ionic strengths is the main problem. We have now planned to use an alternative method based on a polymeric film linked to the silica wall via covalent bonds and covalent binding of the probe protein. Yet, the current results show the feasibility of the sensor for a large range of biological or chemical applications, including measurements for human diseases, process control for the food industry (milk, wine, etc.), and inspection sensors for environmental pollution monitoring.

TFBGs could also be manufactured in photonic crystal fibers (PCF), [17], which will make it possible to extend the potentialities of TFBGs photowritten in standard single-mode fibers by improving their performances. This is due to the increased interaction between the guided optical field and the liquid flowing in the microstructure of holes.

In this context, a French project called Monte-Cristo, supported by the French ministry of research and involving the CEA LIST and the French CNRS, consisted of developing new components and sensors based on microsaturated fibers, FBGs, and

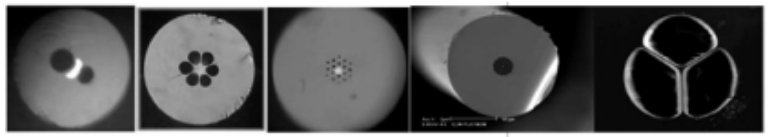

Figure 16. Monte-Cristo Project: Examples of manufactured MOFs.

polymer for selective measurement. The holes are situated in the vicinity of the fiber core and therefore the foreign medium injected into the holes greatly affects the propagation constant (i.e., effective index) as it modifies the interaction between evanescent fields of guided mode and coupled modes. The Bragg wavelength of a FBG written in such a fiber core enables to estimate this change in refractive index. Several microstructurated optical fibers (MOF) have been manufactured during the Monte-Cristo Project up to the final optimized design (three holes) for high refractive index sensitivity, and FBGs have been photo-written into their core (Figure 16) [18].

Several calibrated refractive index liquids (Cargille oils) have been introduced by capillarity into the three fibers in order to measure the refractive index sensitivity of the FBG in this MOF. The effective index of the guided mode increases with the refractive index of the holes. So, when a given liquid reaches the grating, the Bragg resonance experiences a red shift.

Regarding sensing applications, spectra were measured with a 1 pm resolution tunable source. The experimental refractive index resolution is estimated to 4.10^{-3} r.i.u., for the 6-hole MOF, 7.10^{-4} r.i.u. for the two-ring triangular (18 holes) MOF, and 3.10^{-5} r.i.u. for the 3-hole MOF respectively for a value of refractive index close to that of water (~1.33). While, for a value of the refractive index ~1.40 closer to the effective index of the guided mode, the refractive index resolution reaches 2.1 10^{-4} r.i.u. for the 6-hole MOF and for the 8-hole MOF and 6.10^{-6} r.i.u. for the 3-hole MOF (Figure 17) [19].

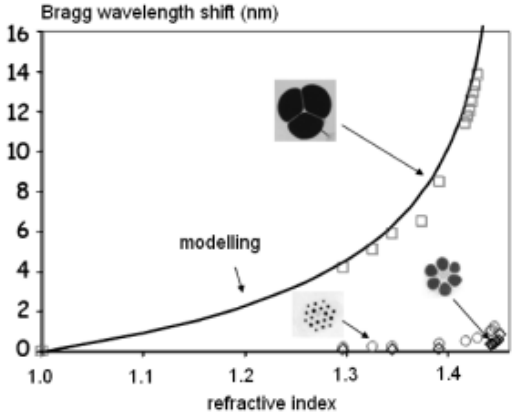

Figure 17. Monte-Cristo Project: FBG measurement and modelling of refractive index for three MOFs.

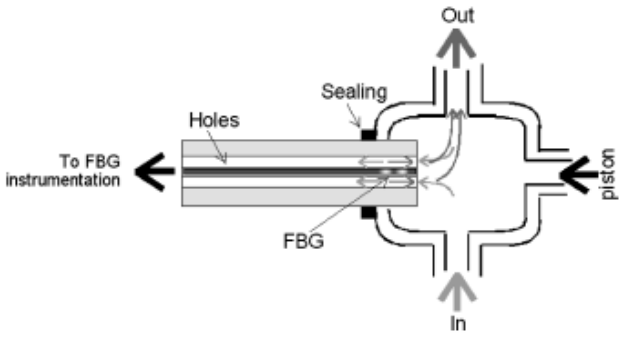

Figure 18. MOF-based refractometer design.

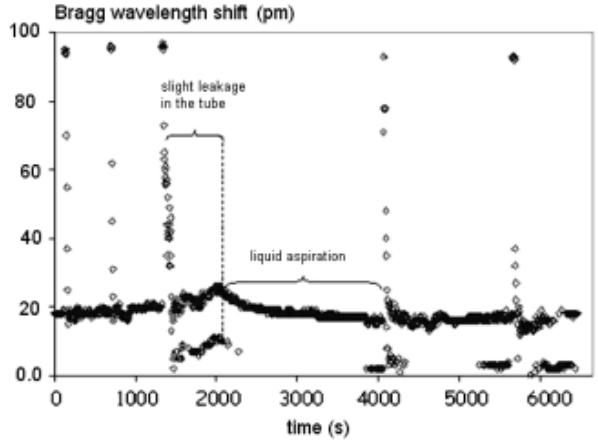

Figure 19. FBG wavelength shift during liquid injection/extraction cycles.

We have also shown that the presence of quinine in a liquid phase solution of printed polymer can be detected with a FBG in the 6-hole fiber. The FBG wavelength shift is about 75 pm between a non-imprinted solution and a quinine printed solution. Nevertheless, this is a very first result, and lack of influence of other molecules (i.e., the selectivity of quinine detection topic) remains to be done.

We have also demonstrated the feasibility of a several times (>4 times) reversible refractometer design at MOF end (Figures 18 and 19).

5. Conclusion

Recent advances in optical fiber metrology obtained at CEA LIST have been reviewed. They involve mainly three dedicated techniques: fiber Bragg grating (FBG) sensors, distributed Brillouin optical time domain reflectometry (B-OTDR), and optically stimulated luminescence (OSL) dosimetry.

Targeted applications are structure monitoring in public works, railway industry, oil and gas, and also the medicine and biomedical sector for which fiber metrology is providing innovative functionalities, seeds of future innovations for sensing industry and of benefit for end-users.

Structural health monitoring (SHM) will play an important role in the future in both civil engineering and transport (aeronautics, railways, etc.). SHM may operate during structure construction (real-time underground monitoring in civil engineering, in situ and real-time monitoring during manufacturing of composite materials) and during service life (on-board SHM). Many civil engineering structures (bridges, dams, etc.) or composite innovative structures need on-line monitoring to prevent failure and ensure safety. Fiber optic metrology is a key technology to achieve this.

Another growing sector is the medical and biomedical fields. Two applications are described in this article: Quality control of the dose in radiotherapy using fiber OSL remote dosimeter and refractometric analysis on compounds and selective antibody identification.

Undoubtedly fiber optic technology is now firmly and durably established in sensing, in spite of a longer lead time than previously expected. This delay is due to several reasons, some of them being: the implicit conservatism in most instrumentation industries, very tight cost margins, and customer-viewed difficulties in accepting product innovation. Moreover, at the early stage of OFS, most sensors aimed at a replacement market, i.e., to compete with traditional instrumentations; this was a difficult challenge. The sensor market being now highly end-user oriented, scientists are more and more aware of end-user needs. More pragmatic than before, these people are now looking for real applications enhancing the new functionalities offered by the OFS(N) technologies.

References

1. Hartog, A. H. 1987. Principle of optical fiber temperature sensors. *Sensor Review* 7(4):197–199.
2. Morey, W. W., Meltz, G., and Glenn, W. H. 1989. Bragg grating temperature and strain sensors. *Optical Fiber Sensor Conference (OFS)'89*, Paris, September, pp. 526–531.
3. Ferdinand, P., and Magne, S. 2000. Applications of optical fiber sensors for nuclear power industry. In: *Handbook on Optical Fiber Sensing Technology—Principle and Applications*, Ch. 26, J. M. Lopez-Higuera (Ed.). John Wiley & Sons, pp. 543–567.
4. Ferdinand, P., Magne, S., Dewynter-Marty, V., Martinez, C., Rougeault, S., and Bugaud, M., 1997. Applications of Bragg grating sensors in Europe. *12th International Conference on Optical Fiber Sensor*. Williamsburg, VA, pp. 14–19, Oct. 28–31.
5. Ferdinand, P., Magne, S., Dewynter-Marty, V., Rougeault, S., and Maurin, L. 2002. Applications of fiber Bragg grating sensors in the composite industry. *MRS Bull.* 27(5):400–407.
6. Ferdinand, P., Dewynter-Marty, V., Maurin, L., Boussoir, J., Rougeault, S., and Magne, S. 2002. FBG-based smart composite applications. D. L. Balageas (Ed.). *1st European Workshop on Structural Health Monitoring (SHM 2002)*, ENS Cachan, France, July 10–12, pp. 552–559.
7. Chang, F.-K. 2007. Structural health monitoring 2007. *Proc. of the 6th Int. Workshop on Structural Health Monitoring*, Stanford, CA, Sept. 11–12, ISBN N° 978-1-932078-71-8.
8. Maurin, L., Boussoir, J., Rougeault, S., Bugaud, M., Ferdinand, P., Landrot, A. G., Grunevald, Y.-H. and Chauvin, T. 2002. FBG-based smart composite bogies for railway applications. *15th Optical Fiber Sensors Conference*, Portland, OR, May 6–10, pp. 91–94, IEEE catalog number: 02EX533, ISBN: 0-7803-7289-1.

9. Laffont, G., Roussel, N., Maurin, L., Boussoir, J., Clogenson, B., Auger, L., Magne, S., and Ferdinand, P. 2005. Wavelength tunable fiber ring laser for high-speed interrogation of fiber Bragg grating sensors. *17th International Conference on Optical Fiber Sensors*, Bruges, Belgium, May 23–27.
10. Maurin, L., Ferdinand, P., Laffont, G., Roussel, N., Boussoir, J., and Rougeault, S. 2007. High speed real-time contact measurements between a smart train pantograph with embedded fiber Bragg grating sensors and its overhead contact line. F. K. Chang (Ed.). *International Conference on Structural Health Monitoring 2007*, Stanford University, Palo Alto, CA, pp. 1808–1815.
11. Magne, S., Boussoir, J., Rougeault, S., Dewynter-Marty, V., Ferdinand, P., and Bureau, L. 2003. Health Monitoring of the Saint-Jean bridge of Bordeaux, France using FBG extensometers. *SPIE 5050, Smart Structures and Materials*, San Diego, CA, pp. 305–316, March 2–6.
12. Magne, S., and Ferdinand, P. 2004. Fiber optic remote gamma dosimeters based on optically stimulated luminescence: State-of-the-art at CEA. *International Radiation Protection Association 11 Conference*, Madrid, Spain, May 23–28.
13. Ranchoux, G., Magne, S., Bouvet, J. P., and Ferdinand, P. 2002. Fiber remote optoelectronic gamma dosimetry based on optically stimulated luminescence of Al_2O_3:C. *Radiation Protection Dosimetry* 100(1–4):255–260.
14. Magne, S., Auger, L., Isambert, A., Bridier, A., Ferdinand, P., and Barthe, J. 2007. Multichannel fiber optic dosimeter based on OSL for dose verification during radiotherapy treatments. *European Workshop on Optical Fiber Sensors (EWOFS 2007)*, Napoli, Italy, pp. 1N-1, 1N-4, July 4–6.
15. Laffont, G., and Ferdinand, P. 2001. Sensitivity of slanted fiber Bragg gratings to external refractive index higher than that of silica. *Electron. Lett.* 37(5):289–290.
16. Laffont, G., and Ferdinand, P. 2001. Tilted short-period fiber-Bragg-grating-induced coupling to cladding modes for accurate refractometry. *Measurement Science and Technology* 12:765–770.
17. Phan Huy, M.-C., Laffont, G., Dewynter-Marty, V., Ferdinand, P., Labonté, L., Pagnoux, D., Roy, Ph., Pagnoux, D., Blanc, W., and Dussardier, B. Tilted fiber Bragg grating photowritten in microstructured optical fiber for improved refractive index measurement. *Optics Express* 14(22):10359–10370.
18. Phan Huy, M.-C., Laffont, G., Frignac, Y., Dewynter-Marty, V., Ferdinand, P., Roy, Ph., Blondy, J.-M., Pagnoux, D., Blanc, W., and Dussardier, B. 2006. Fiber Bragg grating photowriting in microstructured optical fibers for refractive index measurement. *Measurement Science and Technology*, 17(5):992–997.
19. Phan Huy, M.-C., Laffont, G., Dewynter-Marty, V., Ferdinand, P., Roy, Ph., Auguste, J.-L., Pagnoux, D., Blanc, W., and Dussardier, B. 2007. Three-hole microstructured optical fiber for efficient fiber Bragg grating refractometer. *Optics Letters* 32(16):2390–2392.

Biographies

Pierre Ferdinand is head of the Optical Measurement Laboratory at CEA LIST (Atomic Energy Commission, Laboratory of Technologies and Systems Integration, France). His current research includes fiber Bragg grating technologies, optical-fiber sensors and sensor networks for advanced structure health monitoring. He received an MS degree in Physics in 1978 from the Univ. Pierre et Marie Curie (Paris VI), and the Diplôme d'Etudes Approfondies in plasma physics in 1980 from the Univ. of Paris XI, in Orsay. In 1982, he earned the Ph.D in physics from the Univ. of Paris XI, and in 1990 he received its State Ph.D (*Doctorat d'Etat es Sciences*) from the Univ. of Nice. From 1980 to 1992, P. Ferdinand worked at the R&D Division of EDF. During this time, he focused mainly on optical-sensing topics such as stabilized optical sources and OFS. Ferdinand holds 20 patents and is the author of one scientific book and several book chapters as

co-editor, and approximately 80 research publications on OFS and related subjects. He is a fellow of both the French and the European Optical Societies (SFO and EOS). He is also a member of the International OFS Conference technical committee as well as the European Workshop on Optical Fiber Sensors' committee.

Sylvain Magne is a senior engineer with CEA LIST. His current research includes fiber Bragg grating (FBG) sensors and networks for advanced structure monitoring and sensing and optically stimulated luminescence (OSL) dosimetry for radiation protection and radiotherapy applications. He received the diploma of technician from the Institut Universitaire de Technologie Mesures Physiques (Grenoble, France) in 1986 and the Diploma of Engineer in Physics from the Institut National Polytechnique de Grenoble in 1989, as well as the Diplôme d'Etudes Approfondies in Instrumentation from Université Joseph Fourier (Grenoble) in 1989. He received his Ph.D degree in optics–optoelectronics from the University of Saint-Etienne, France, in 1993. From 1990 to 1993, he worked at LETI (Electronics and Information Technology Laboratory, CEA) in Saclay, France, jointly with the Signal Processing and Instrumentation Laboratory of the CNRS (National Center for Scientific Research) on rare-earth-doped fiber lasers and spectroscopy. He is the author of approximately 15 publications, 30 conference papers and is also author or co-author of eleven patents. He is a fellow of the Société Française d'Optique and of the European Optical Society.

Guillaume Laffont is an engineer from the Ecole Nationale Supérieure de Physique de Strasbourg – ENSPS. He completed a Ph.D in physics and optics in 2001 at the Université de Lille, France, for research on the photo-writing, modelling, and sensing application of tilted FBGs. His current research includes the development of FBG-based sensors and systems. He is involved in the development of tuneable sources, of innovative FBG components and in the design of photosensitive photonic crystal fiber. He also works on the use of bio-functionalized FBG-based transducers for biochemical applications. He is author and co-author of 8 scientific papers and 17 conference contributions. He also holds 6 patents.

Véronique Dewynter is a senior engineer graduated from ENSSAT, the Ecole Nationale Supérieure des Sciences Appliquées et de Technologie in Lannion, France, with a specialization in Optronics. She joined the Optical Measurement Laboratory of the CEA LIST (Atomic Energy Commission, Laboratory of Technologies and Systems Integration, France) in 1992 to work on optical fiber sensors. Her current research includes Fiber Bragg Grating (FBG) sensors, Brillouin optical time domain reflectometry (B-OTDR), for structure monitoring. She worked on several national and international projects dealing with underground and tunnelling monitoring during construction, civil engineering, and composite materials.

Laurent Maurin, Civil Engineer of the École des Mines de Nancy, is also graduated from the "Centre for Material Forming" of the École des Mines de Paris. In 1995, he joined the Alcatel's single-mode fiber unit in northern France, as a process and development engineer, and get involved in MCVD, draw and measurements processes. In 1999, Laurent Maurin joined the Optical Measurements Laboratory at CEA Saclay, and is now currently involved in projects dealing with several aspects of FBG measurements and sensors. L. Maurin currently holds 9 patents dealing with optical fiber manufacturing, measurements, and sensors.

Cécile Prudhomme was graduated, in 2001, as an engineer from ENSTB, the Ecole Nationale Supérieure des Télécommunications de Bretagne in Brest, France, with a specialization in Optics. In 2003, she joined the CEA LIST, Optical Measurement

Laboratory, as a Research engineer, focusing on optical fiber sensors and fiber Bragg grating-based sensors and systems.

Nicolas Roussel is an engineer who has been working on the fiber Bragg grating sensors interrogation units in the Optical Measurements Laboratory at CEA LIST for six years. In 2001, he received the diploma of engineer in optical metrology and instrumentation from the Conservatoire National des Arts et Metiers in Paris. He previously worked on several projects (SMITS, etc.) and works currently on the CATIEMON European project to develop the optical FBG-based instrumentation, including Optoelectronics, hardware and software development as well as components qualification.

Marie Giuseffi was graduated, in 2003, as an engineer from ENSSAT, the Ecole Nationale Supérieure des Sciences Appliquées et de Technologie in Lannion, France, with a specialization in Optronics. From 2003 to 2006, she was with the SME Fogale-Nanotech, in charge of low-coherence optical interferometer development. Mid-2006, she joined the French SME, SITES S.A., where she specialized in instrumentation for civil engineering applications. Since 2007, she is a Research engineer at the CEA LIST, Optical Measurement Laboratory, focusing on optical fiber sensors and fiber Bragg grating-based sensors and systems.

Séverine Maguis was graduated in 2004 as an engineer from the Ecole Supérieure d'Optique (ESO) in Orsay, France. She is currently preparing a Ph.D at CEA, LIST, Optical Measurement Laboratory, focusing on fiber Bragg grating-based biosensors.